Dirac and Majorana edge states in graphene and topological superconductors

Akhmerov, A.R.

Chapter 12

Probing Majorana edge states with a flux qubit

12.1 Introduction

Chiral Majorana fermion edge states were originally predicted to exist in the $5/2$ fractional quantum Hall plateau [5]. These edge states support not only neutral fermionic excitations but also more exotic edge vortices. A single edge vortex corresponds to a π phase shift to all fermions situated to one side of it [182, 242, 244]. Two edge vortices may either fuse into an edge fermion or annihilate each other, with the outcome depending on the preceding evolution of the system. In other words, the edge theory (together with the corresponding bulk theory) possesses non-Abelian statistics [6, 9, 129, 139]. This unusual physics and its potential applications to topological quantum computation are the reasons why the Majorana edge states have attracted much attention recently [8, 174–176, 240, 256].

Similar non-Abelian anyons and their corresponding edge states appear in superconducting systems as well. Initially it was discovered that p-wave superconductors support non-Abelian anyons in the bulk and chiral Majorana edge states [6, 234]. Later it was shown that depositing a conventional s-wave superconductor on the surface of a topological insulator while breaking time-reversal symmetry provides an alternative route to realize these non-Abelian states [130, 144, 145]. Alternative proposals include substituting the topological insulator by a two-dimensional electron gas with spin-orbit coupling [131, 228, 257] or by a half-metal [258, 259]. The realizations of Majorana edge states using s-wave superconductors have the following advantages: first, they rely on combining simple, well-studied ingredients. Second, the materials do not have to be extremely pure unlike samples needed to support the fractional quantum Hall edge states. Finally, the superconducting implementations of Majorana fermions may feature a larger bulk excitation gap and may therefore be operated at higher temperatures.

The downside of the superconducting implementations of Majorana edge states is the lack of means to manipulate edge vortices [144, 145]. Different from the 5/2 fractional quantum Hall state, the edge vortices are not coupled to charge and thus cannot be controlled by applying voltages [260]. Therefore, the standard proposal to probe the

edge vortices in superconducting systems is to inject fermion excitations into the edge, to let them split into edge vortices, and finally to conclude about the behavior of the edge vortices from the detection of the fermion excitations after the subsequent fusion of edge vortices [144, 145, 260, 261].

In this chapter, we propose a more direct way to manipulate and measure edge vortices using a flux qubit consisting of a superconducting ring interrupted by a Josephson junction [143, 262]. Our main idea is based on the following observations: first, an edge vortex is created when a superconducting vortex crosses the edge. Second, the motion of the superconducting vortices can be fully controlled by a flux qubit, since by applying a flux bias to the qubit one can tune the energy cost for a vortex being present in the superconducting ring [262]. In this way, attaching a flux qubit to a system supporting Majorana edge states allows to directly create, control, and measure edge vortices without relying on splitting and fusing fermionic excitations.

We note that our proposal is not necessarily advantageous for the purposes of topological quantum computing since quantum computing with Majorana fermions may even be realized without ever using edge states [143, 210, 211]. Instead the aim of our investigation is to develop a better tool for probing the fractional excitations of the edge theory.

The chapter is organized as follows. In Sec. 12.2, we discuss a schematic setup of a system where a pair of chiral Majorana fermion edge modes couple to a flux qubit as a probe of the edge states and briefly list our main findings. In Sec. 12.3, we review the connection between the one-dimensional critical transverse-field Ising model and Majorana fermion modes. We identify the vortex tunneling operators between two edge states as the disorder fields of the Ising model, and subsequently derive an effective Hamiltonian for the flux qubit coupled to Majorana modes. In Sec. 12.4, we provide the necessary formalism for evaluating the expectation values for the flux qubit state and qubit susceptibilities. In Sec. 12.5 and Sec. 12.6, we compute the qubit expectation values and the two-point qubit correlation functions in the presence of the edge state coupling, and use these results to derive the qubit susceptibility. In Sec. 12.7, we analyze higher order corrections to correlation functions of the qubit state. We summarize our results in Sec. 12.8. Additionally, we include some mathematical details in two Appendices.

12.2 Setup of the system

In this work, we consider the following setup: a strip of *s*-wave superconductor is deposited on the surface of either a three-dimensional topological insulator or a semiconductor with strong spin-orbit coupling and broken time-reversal symmetry (or any other superconducting setup supporting Majorana edge states). As depicted in Fig. 12.1, a pair of counter-propagating Majorana fermion edge modes appears at the two opposite edges of the superconductor [144, 145]. To avoid mixing between counter-propagating edge states, the width of the superconductor should be much larger than the superconducting coherence length $\hbar v_F/\Delta$. Here and in the following, v_F denotes the Fermi velocity of the topological insulator (semiconductor) and Δ the proximity-induced superconduct-

ing pair-potential. In order to avoid mixing of the two counter-propagating edge modes at the ends of the sample, we require either the length of the superconducting strip to be longer than the dephasing length or metallic leads to be attached to the ends of the sample.

A flux qubit, consisting of a superconducting ring with a small inductance interrupted by a Josephson junction, is attached to the heterostructure supporting the Majorana edge modes, as shown in Fig. 12.1. By applying an external flux, the two classical states of the superconducting ring corresponding to the phase difference of 0 and 2π across the junction can be tuned to be almost degenerate [262]. In this regime, the flux qubit can be viewed as a quantum two-level system with an energy difference ε (which we choose to be positive) between the states $|0\rangle$ and $|2\pi\rangle$ and a tunneling amplitude δ between them. The transition between the two qubit states is equivalent to the process of a vortex tunneling through the Josephson junction in or out of the superconducting ring. For convenience, we will refer to the Hilbert space spanned by the qubit states $|0\rangle$ and $|2\pi\rangle$ as a spin-$1/2$ system. For example, we are going to call the Pauli matrices $\sigma^{x,y,z}$ acting on the qubit states the qubit spin.

A vortex tunneling through the weak link in the superconductor from one edge to the other is a phase slip of 2π of the superconducting phase difference at the tunneling point. Due to this event, all fermions to one side of the weak link gain a phase of π. As will be shown below, the vortex tunneling operator can be identified with the operator of the disorder field of a one-dimensional critical Ising model onto which the Majorana edge modes can be mapped.

Since vortex tunneling events couple the qubit spin to the Majorana edge modes, we expect various observables of the qubit to carry signatures of this coupling. The main theory parameter that we are after is the scaling dimension $\Delta_\mu = 1/8$ of the edge vortex operator (disorder field). Our main results apply to the regime when vortex tunneling is weak $\varepsilon \gg \delta$.

We find that the reduction of the spin expectation value in the z-direction due to the vortex tunneling acquires a nontrivial scaling exponent

$$1 - \langle \sigma^z \rangle \propto \frac{\delta^2}{\varepsilon^{2-2\Delta_\mu}} = \frac{\delta^2}{\varepsilon^{7/4}}. \tag{12.1}$$

Similarly, the spin expectation value along the x-direction is proportional to $\varepsilon^{2\Delta_\mu - 1} = \varepsilon^{-3/4}$ thereby probing the scaling dimension of the disorder field.

Besides the static measurements of spin expectation values, the frequency-dependent susceptibilities, that characterize the response of the polarization of the qubit spin, also provide information about the Majorana edge states. Experimentally they can be determined by measuring the response of the qubit when an oscillating magnetic field is coupled to the qubit that changes either the energy difference ε or the tunneling amplitude δ. The frequency dependence of the susceptibilities exhibits a non-Lorentzian resonant response around the frequency $\omega \approx \varepsilon$ (here and in the following, we set $\hbar = 1$). It is modified by the coupling to the Majorana edge states and shows the scaling behavior

$$|\chi(\omega)| \propto \frac{1}{|\omega - \varepsilon|^{1-2\Delta_\mu}} = \frac{1}{|\omega - \varepsilon|^{3/4}}, \tag{12.2}$$

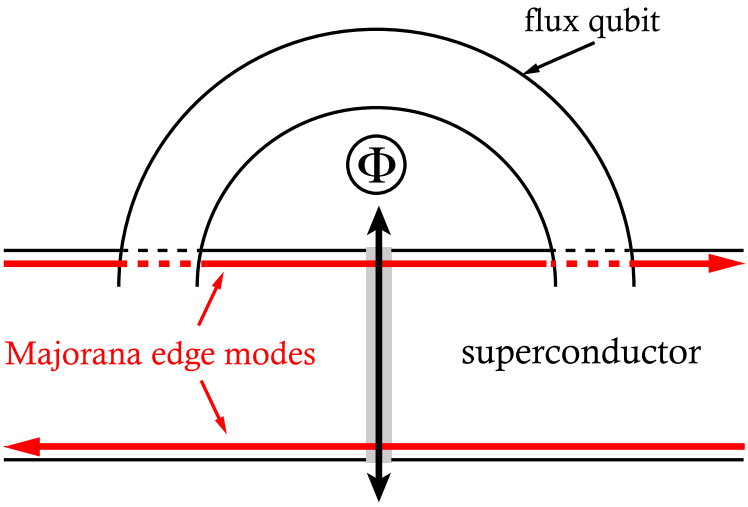

Figure 12.1: Schematic setup of the Majorana fermion edge modes coupled to a flux qubit. A pair of counter-propagating edge modes appears at two opposite edges of a topological superconductor. A flux qubit, that consists of a superconducting ring and a Josephson junction, shown as a gray rectangle, is attached to the superconductor in such a way that it does not interrupt the edge states flow. As indicated by the arrow across the weak link, vortices can tunnel in and out of the superconducting ring through the Josephson junction.

as long as $\varepsilon \gg |\omega - \varepsilon|$, and the distance $|\omega - \varepsilon|$ from the resonance is larger than the width of the resonance. The phase change of susceptibility at the resonance $\delta\phi = 3\pi/4$ is different from the π phase change for a usual oscillator. The origin of the extra $\pi/4$ phase shift is the Abelian part of the statistical angle of the vortex excitations [8].

12.3 Edge states and coupling to the qubit

12.3.1 Coupling of the flux qubit to the edge states

The flux qubit has two low energy states, corresponding to a phase difference $\phi = 0$ or $\phi = 2\pi$ across the Josephson junction at $x = x_0$. The Hamiltonian of the qubit is given by

$$H_Q = -\frac{\varepsilon}{2}\sigma^z - \frac{\delta}{2}e^{i\alpha}\sigma^+ - \frac{\delta}{2}e^{-i\alpha}\sigma^-. \tag{12.3}$$

The energy difference ε can be tuned by applying an external flux to the qubit while the tunneling amplitude $\delta > 0$ can be manipulated by changing the Josephson coupling of the junction [262]. The tunneling phase α is proportional to the charge induced on the sides of the junction and its fluctuations are the main source of qubit decoherence. For

simplicity we neglect the charge noise so that we can assume that α is static and set it to zero without loss of generality. The qubit Hamiltonian now reads

$$H_Q = -\frac{\varepsilon}{2}\sigma^z - \frac{\delta}{2}\sigma^x. \tag{12.4}$$

When there is no phase difference across the Josephson junction ($\phi = 0$), the Hamiltonian of the chiral Majorana modes appearing at the edges of the superconductor, as shown in Fig. 12.1, reads

$$H_{\mathrm{MF}} = \frac{i v_M}{2} \int \frac{dx}{2\pi} [\psi_d(x)\partial_x \psi_d(x) - \psi_u(x)\partial_x \psi_u(x)], \tag{12.5}$$

where v_M is the velocity of the Majorana modes, and $\psi_u(x)$ and $\psi_d(x)$ are the Majorana fermion fields at the upper and lower edges of the superconductor in Fig. 12.1. The sign difference between the terms containing ψ_u and ψ_d is due to the fact that the modes are counter-propagating. The Majorana fermion fields obey the anti-commutation relations

$$\begin{aligned} &\{\psi_u(x), \psi_u(x')\} = \{\psi_d(x), \psi_d(x')\} = 2\pi\delta(x - x'), \\ &\{\psi_u(x), \psi_d(x')\} = 0. \end{aligned} \tag{12.6}$$

A vortex tunneling through the weak link at $x = x_0$ advances the phase of each Cooper pair in the region $x \leq x_0$ by 2π. For Majorana fermions, just like any other fermions, this results in phase shift of π. The effect of this phase shift is a gauge transformation

$$H_{\mathrm{MF}} \mapsto P H_{\mathrm{MF}} P, \tag{12.7}$$

where the parity operator P is given by

$$P = \exp\Big[i\pi \int_{-\infty}^{x_0} dx\, \rho_e(x)\Big], \tag{12.8}$$

with the fermion density $\rho_e(x) = [\pi\delta(x) + i\psi_u(x)\psi_d(x)]/2\pi$. The relation between the phase slip and the parity operator was discussed and used in previous work focusing on the $5/2$ fractional quantum Hall state [242, 244, 256].

Combining the Hamiltonian of the Majorana edge states (12.5, 12.7) with the qubit Hamiltonian (12.4), we get the full Hamiltonian of the coupled system in the basis of $|0\rangle$ and $|2\pi\rangle$:

$$\mathcal{H} = \begin{pmatrix} H_{\mathrm{MF}} & 0 \\ 0 & P H_{\mathrm{MF}} P \end{pmatrix} + H_Q. \tag{12.9}$$

The first part of Hamiltonian represents the chiral Majorana edge states coupled to the phase slip of the superconductor while the second part is the bare flux qubit Hamiltonian.

Because the parity operator (12.8) is highly nonlocal if expressed in terms of Majorana fermions, it is desirable to map the Majorana modes on a system where the vortex tunneling event becomes a local operator. To this end, we establish the equivalence of the chiral Majorana edge modes with the long wavelength limit of the one-dimensional transverse-field Ising model at its critical point [246, 263].

12.3.2 Mapping on the critical Ising model

The lattice Hamiltonian of the Ising model at the critical point is given by [246, 263]:

$$H_I = -J \sum_n (s_n^x s_{n+1}^x + s_n^z), \tag{12.10}$$

where s_n^α are the spin-$1/2$ operators at site n. With the Jordan-Wigner transformation,

$$\begin{aligned} s_n^+ =& c_n \exp(i\pi \sum_{j<n} c_j^\dagger c_j), \\ s_n^- =& c_n^\dagger \exp(i\pi \sum_{j<n} c_j^\dagger c_j), \quad s_n^z = 1 - 2c_n^\dagger c_n, \end{aligned} \tag{12.11}$$

the Ising model (12.10) can be cast in terms of fermions as

$$H_I = J \sum_n [(c_n - c_n^\dagger)(c_{n+1} + c_{n+1}^\dagger) + c_n^\dagger c_n - c_n c_n^\dagger]. \tag{12.12}$$

Here $s_i^\pm \equiv (s_i^x \pm i s_i^y)/2$ obey the usual onsite spin commutation relations while the fermions operators $c_i^\dagger$ and c_i obey canonical anti-commutation relations.

For each fermion, we introduce a pair of Majorana operators $\psi_n = \psi_n^\dagger$ and $\bar{\psi}_n = \bar{\psi}_n^\dagger$ such that

$$c_n = \frac{e^{-i\pi/4}}{2}(\psi_n + i\bar{\psi}_n). \tag{12.13}$$

The Majorana fermions satisfy the Clifford algebra

$$\{\psi_m, \psi_n\} = \{\bar{\psi}_m, \bar{\psi}_n\} = 2\delta_{mn}, \qquad \{\psi_m, \bar{\psi}_n\} = 0. \tag{12.14}$$

In terms of the Majorana operators, the Hamiltonian (12.12) assumes the form

$$H_I = -\frac{iJ}{2} \sum_n (\psi_n \psi_{n+1} - \bar{\psi}_n \bar{\psi}_{n+1} + \psi_n \bar{\psi}_{n+1} - \bar{\psi}_n \psi_{n+1} - 2\psi_n \bar{\psi}_n). \tag{12.15}$$

In the long wavelength limit, the Hamiltonian (12.15) reduces to (12.5) with the identification of the continuum Majorana operators

$$\psi_u(x) \mapsto \sqrt{\frac{\pi}{a}}\psi_n, \quad \psi_d(x) \mapsto \sqrt{\frac{\pi}{a}}\bar{\psi}_n, \quad x \mapsto na \tag{12.16}$$

and the velocity $v_M \mapsto 2Ja$. To complete the mapping, the bandwidth of the Ising model should be related to the cutoff energy Λ of the linear dispersion of the Majorana edge states, $\Lambda \mapsto J$. Thereby, a pair of counter-propagating Majorana edge states, $\psi_u(x)$ and $\psi_d(x)$, can be mapped on the low energy sector of the one-dimensional transverse-field Ising model at its critical point.

For the parity operator (12.8), we obtain a representation in terms of the Ising model with the following procedure: we first discretize $\int^{x_0} dx\, \rho_e(x)$ using the mapping (12.16) and identify $x_0 \equiv n_0 a$ as a lattice point on the Ising model. Thereafter, we obtain an expression for the vortex tunneling operator P in terms of the Ising model

$$P \mapsto \exp\Big(i\pi \sum_{j\le n_0} c_j^\dagger c_j\Big) = \prod_{j\le n_0} s_j^z \equiv \mu^x_{n_0+1/2}, \tag{12.17}$$

by using Eq. (12.13) and the Jordan-Wigner transformation (12.11). Here, μ^x is the disorder field of the Ising model, i.e., the dual field of the spin field [246, 263–265]. The Ising Hamiltonian has a form identical to Eq. (12.10) when expressed through μ operators,

$$H_I = -J \sum_n (\mu^x_{n-1/2}\mu^x_{n+1/2} + \mu^z_{n+1/2}), \tag{12.18}$$

with $\mu^z_{n+1/2} = s^z_n s^z_{n+1}$.[1] We see that the parity operator is indeed a local operator in the dual description of the Ising model. After mapping on the Ising model Eq. (12.7) becomes (here and in the following, we use the shortcut notation $\mu = \mu^x$)

$$P H_{\rm MF} P \mapsto \mu_{n_0+1/2}\, H_I\, \mu_{n_0+1/2}, \tag{12.19}$$

and the full Hamiltonian of Majorana edge states and the flux qubit (12.9) maps onto

$$\mathcal{H} \mapsto \mathcal{H}_I = \begin{pmatrix} H_I & 0 \\ 0 & \mu_{n_0+1/2}\, H_I\, \mu_{n_0+1/2} \end{pmatrix} + H_Q. \tag{12.20}$$

Finally, an additional unitary transformation

$$\mathcal{H}_I \mapsto V \mathcal{H}_I V^\dagger, \tag{12.21}$$

$$V = V^\dagger = \begin{pmatrix} 1 & 0 \\ 0 & \mu_{n_0+1/2} \end{pmatrix}, \tag{12.22}$$

yields

$$\mathcal{H}_I = H_I - \frac{\varepsilon}{2}\tau^z - \frac{\delta}{2}\tau^x \mu_{n_0+1/2}. \tag{12.23}$$

Here, τ^i are the Pauli matrices acting in the Hilbert space spanned by the states $|0\rangle$ and $\mu_{n_0+1/2}|2\pi\rangle$. The operators of the qubit spin can be expressed through $\tau^{x,y,z}$ as

$$\sigma^z = \tau^z, \quad \sigma^x = \tau^x \mu_{n_0+1/2}, \quad \sigma^y = \tau^y \mu_{n_0+1/2}. \tag{12.24}$$

We use the Hamiltonian in the form of Eq. (12.23) and the qubit spin operators (12.24) in the rest of the chapter.

[1] In the present work, the Jordan-Wigner transformation (12.11) is introduced for the Ising spin fields s^x. If the transformation is introduced for the disorder field, as in Refs. [241] and [248], one should interchange the Ising spin field and the disorder field in our discussion.

The way of identifying *two* edge Majorana states with a *complete* transverse field Ising model presented above is different from the one commonly used in preceding research. Usually, the *chiral part* of the Ising model is identified with a *single* Majorana edge [182, 260]. The advantages of our method are the possibility to write a complete Hamiltonian of the problem and simplified book-keeping, while its drawback is the need for the right-moving edge and the left-moving edge to have the same geometries. Overall the differences are not important and both methods can be used interchangeably.

12.4 Formalism

To probe the universal properties of Majorana edge states, the energy scales of the qubit should be much smaller than the cutoff scale of the Ising model, $\varepsilon, \delta \ll \Lambda$. In the weak coupling limit $\varepsilon \gg \delta$, we construct a perturbation theory in δ/ε by separating the Hamiltonian $\mathcal{H}_I = \mathcal{H}_0 + V$ into an unperturbed part and a perturbation

$$\mathcal{H}_0 = H_I - \frac{\varepsilon}{2}\tau^z, \qquad V = -\frac{\delta}{2}\tau^x \mu. \tag{12.25}$$

Without loss of generality we set $\varepsilon > 0$, so that the ground state of the unperturbed qubit is $|0\rangle$. For brevity we omit the spatial coordinate of the μ operator in the following since it is always the same in the setup that we consider.

We use the interaction picture with time-dependent operators

$$\mathcal{O}(t) = e^{i\mathcal{H}_0 t}\mathcal{O}e^{-i\mathcal{H}_0 t}. \tag{12.26}$$

The perturbation $V(t)$ in this picture is given by

$$V(t) = -\frac{\delta}{2}\mu(t)[\tau^+(t) + \tau^-(t)], \tag{12.27}$$

where $\tau^\pm(t) = e^{\mp i\varepsilon t}\tau^\pm$ are the time-dependent raising and lowering operators. The structure of the raising and lowering operators leads to physics similar to the Kondo and Luttinger liquid resonant tunneling problems [182, 237, 266].

In the calculation we need the real-time two-point and four-point correlation functions of μ in the long-time limit $\Lambda|t - t'| \gg 1$. The two-point correlation function is

$$\langle \mu(t)\mu(t')\rangle = \frac{e^{-i\,\mathrm{sgn}(t-t')\pi/8}}{\Lambda^{2\Delta_\mu}|t-t'|^{2\Delta_\mu}}, \tag{12.28}$$

where $\mathrm{sgn}(x)$ denotes the sign of x, and $\Delta_\mu = 1/8$ the scaling dimension of the μ field [251, 252]. The phase shift $\pi/8$ of the two-point correlator is the Abelian part of the statistical angle for the Ising anyons braiding rules [8]. Correlation functions involving combination of multiple fields can be obtained via the underlying Ising conformal field theory or via a bosonization scheme [241, 248, 251, 252]. The expression for the four-point correlation function is given in App. 12.A due to its length. For brevity we will

measure energies in units of Λ and times in units of $1/\Lambda$ in the following calculation and restore the dimensionality in the final result.

We are interested in observables of the flux qubit: the spin expectation values and the spin susceptibilities. We use time-dependent perturbation theory to calculate these quantities [267]. This method is straightforward because of the simple form of the perturbing Hamiltonian (12.27) in terms of raising and lowering operators.

Assuming that the system is in the unperturbed ground state at time $t_0 \to -\infty$, the expectation value of a qubit spin operator $\sigma^\alpha(t)$ is expressed through the S-matrix $S(t,t')$,

$$\langle \sigma^\alpha(t)\rangle = \langle S(t,t_0)^\dagger \sigma^\alpha(t) S(t,t_0)\rangle_0, \tag{12.29}$$

$$S(t,t') = \mathcal{T}\exp\left(-i\int_{t'}^{t} V(s)ds\right),\ t > t'. \tag{12.30}$$

Here, $\mathcal{T}$ is the time-ordering operator and $\langle\cdot\rangle_0$ is the expectation value with respect to the unperturbed ground state. Similarly, the two-point correlation functions of the qubit spin are given by

$$\langle \sigma^\alpha(t)\sigma^\beta(0)\rangle = \langle S^\dagger(t,t_0)\sigma^\alpha(t)S(t,0)\sigma^\beta(0)S(0,t_0)\rangle_0. \tag{12.31}$$

The perturbative calculation for both the expectation values and correlation functions is done by expanding the S-matrices in V order by order. This procedure is equivalent to the Schwinger-Keldysh formalism with the expansion of S and $S^\dagger$ corresponding to insertions on the forward and backward Keldysh contour.

According to linear response theory, the susceptibility is given by the Fourier transform of the retarded correlation function of the qubit [267]:

$$\begin{aligned}\chi_{\alpha\beta}(\omega) &= i\int_0^\infty dt\, e^{i\omega t}\langle[\sigma^\alpha(t),\sigma^\beta(0)]\rangle_c \\ &= -2\int_0^\infty dt\, e^{i\omega t}\,\mathrm{Im}\langle\sigma^\alpha(t)\sigma^\beta(0)\rangle_c,\end{aligned} \tag{12.32}$$

where $\langle\cdot\rangle_c$ denotes the cumulant,

$$\langle \sigma^\alpha(t)\sigma^\beta(0)\rangle_c = \langle \sigma^\alpha(t)\sigma^\beta(0)\rangle - \langle\sigma^\alpha(t)\rangle\langle\sigma^\beta(0)\rangle, \tag{12.33}$$

and we have used $\langle\sigma^\beta(0)\sigma^\alpha(t)\rangle_c = \langle\sigma^\alpha(t)\sigma^\beta(0)\rangle_c^*$. We see that in order to calculate the susceptibilities only the imaginary part of the correlation functions for $t > 0$ is required.

12.5 Expectation values of the qubit spin

In this section, we calculate the expectation values of the qubit spin due to coupling with the Majorana edge states to the lowest non-vanishing order. Using the identity

$$\sigma^z = 1 - 2\sigma^-\sigma^+, \tag{12.34}$$

we obtain

$$\langle\sigma^z\rangle - \langle\sigma^z\rangle^{(0)} = -2\langle\sigma^-\sigma^+\rangle = -2\langle\tau^-\tau^+\rangle, \tag{12.35}$$

since $\langle\sigma_z\rangle^{(0)} = 1$.

The first non-vanishing correction in the perturbative calculation of $\langle\sigma^-\sigma^+\rangle$ is of second order in V. By expanding S and $S^\dagger$ in Eq. (12.29), we obtain

$$\langle\tau^-\tau^+\rangle^{(2)} = \int_{-\infty}^{0} dt_1 \int_{-\infty}^{0} dt_2\, I^z, \tag{12.36}$$
$$I^z = \langle V(t_2)\tau^-\tau^+ V(t_1)\rangle_0.$$

The integrand I_z originates from the first order expansion of both S and $S^\dagger$. The second order contributions from the same S- or $S^\dagger$-matrix vanish due to the structure of V in the qubit spin space.

Substituting (12.27) and (12.28) into the integrand I^z yields

$$I^z = \frac{\delta^2 e^{i\varepsilon(t_1-t_2)-i\,\mathrm{sgn}(t_2-t_1)\pi/8}}{4|t_2-t_1|^{2\Delta_\mu}}. \tag{12.37}$$

By evaluating the integral in Eq. (12.36), we find

$$\langle\sigma^z\rangle^{(2)} = -2\langle\tau^-\tau^+\rangle^{(2)} = -\frac{3\Gamma(\frac{3}{4})\delta^2}{8\varepsilon^{2-2\Delta_\mu}}, \tag{12.38}$$

where $\Gamma(x)$ denotes the Gamma function.

The expectation value of σ^x in the unperturbed ground state vanishes. The first non-vanishing contribution to $\langle\sigma^x\rangle$ arises to first order in δ/ε. Expanding S and $S^\dagger$ in Eq. (12.29) to the first order yields

$$\langle\sigma^x\rangle^{(1)} = \int_{-\infty}^{0} dt_1\, I^x, \tag{12.39}$$
$$I^x = -i\,\langle[\tau^x\mu(0), V(t_1)]\rangle_0 = \frac{\sin(-\varepsilon t_1 + \frac{\pi}{8})\delta}{|t_1|^{2\Delta_\mu}}$$

after substituting σ^x from Eq. (12.24) and employing the two point correlator, Eq. (12.28). Evaluating (12.39), we find

$$\langle\sigma^x\rangle^{(1)} = \frac{\Gamma(\frac{3}{4})\delta}{\varepsilon^{1-2\Delta_\mu}}. \tag{12.40}$$

Finally, $\langle\sigma^y\rangle = 0$ to all orders in perturbation theory since the Hamiltonian is invariant under $\sigma^y \mapsto -\sigma^y$.

12.6 Correlation functions and susceptibilities of the flux qubit spin

Since we are interested in the behavior of susceptibilities at frequencies close to the resonance $\omega \approx \varepsilon$, we only need to obtain the long-time asymptotic of the correlation

functions of the qubit spin. Using (12.24) and (12.28), we immediately obtain that

$$\langle \sigma^x(t)\sigma^x(0)\rangle_c = \frac{e^{-i\varepsilon t - i\pi/8}}{t^{2\Delta_\mu}}, \tag{12.41}$$

is non-vanishing to zeroth order. This is due to the fact that flipping the qubit spin automatically involves creation of an edge vortex, and σ^x is exactly the spin flip operator. In the same manner, one obtains that $\langle \sigma^y(t)\sigma^y(0)\rangle_c = \langle \sigma^x(t)\sigma^x(0)\rangle_c$ to zeroth order.

Concentrating next on the mixed correlator, the relations (12.24) and (12.34) yield

$$\langle \sigma^x(t)\sigma^z(0)\rangle_c = -2\langle \mu(t)\tau^x(t)\tau^-(0)\tau^+(0)\rangle_0. \tag{12.42}$$

The leading non-vanishing term in this correlation function is of first order in δ and given by

$$\langle \sigma^x(t)\sigma^z(0)\rangle_c^{(1)} = -\frac{\delta}{\varepsilon}\langle \sigma^x(t)\sigma^x(0)\rangle_c. \tag{12.43}$$

in the long-time limit.

The leading order contribution to $\langle \sigma^z(t)\sigma^z(0)\rangle_c$ can be evaluated using (12.28) with expansions of S and $S^\dagger$ to second order in δ. In the long-time limit, the leading contribution of the correlation function is given by

$$\langle \sigma^z(t)\sigma^z(0)\rangle_c^{(2)} = \frac{\delta^2}{\varepsilon^2}\langle \sigma^x(t)\sigma^x(0)\rangle_c. \tag{12.44}$$

Correlators containing a single σ^y vanish because of the invariance under $\sigma^y \mapsto -\sigma^y$. We see that all the non-vanishing two-point correlation functions are the same up to overall prefactors. Therefore, we will focus on $\langle \sigma^x(t)\sigma^x(0)\rangle_c$ in the following.

12.6.1 Energy renormalization and damping

The coupling of the flux qubit to the continuum Majorana edge states can be thought of as a two-level system coupled to an environment via the interaction (12.27). This coupling leads to self-energy corrections Σ for the qubit Hamiltonian

$$\mathcal{H}_0 \mapsto \mathcal{H}_0 + \Sigma, \quad \Sigma = \begin{pmatrix} \Sigma_{\uparrow\uparrow} & \Sigma_{\uparrow\downarrow} \\ \Sigma_{\downarrow\uparrow} & \Sigma_{\downarrow\downarrow} \end{pmatrix}, \tag{12.45}$$

that effectively shifts the energy spectrum and can also induce damping [268]. Since we are mainly interested in qubit observables, we neglect the structure of Σ in the space of Ising spins.

To second order, the self-energy correction for two spin states can be written [268] in terms of the perturbed Hamiltonian (12.25) as:

$$\Sigma_{\alpha\beta} = \langle \alpha; 0|V + V(E_\alpha + i0^+ - \mathcal{H}_0)^{-1}V|0;\beta\rangle, \tag{12.46}$$

where E_α is the energy for the spin-α $=\uparrow,\downarrow$ qubit states and $|\alpha;0\rangle$ indicates that the Ising model is in its ground state with spin-α for the qubit state. Due to the structure of

the Hamiltonian (12.25), the first order correction to the self-energy vanishes. Additionally, the off-diagonal self-energy corrections vanish also to second order.

By inserting a complete set $\sum_{E_I,\beta} |E_I;\beta\rangle\langle\beta;E_I| = 1$ of the Hilbert space of $\mathcal{H}_0$ with E_I denoting the complete set of eigenstates with energy E_I for the Ising sector, the diagonal elements of the self-energy become

$$\Sigma_{\alpha\alpha} = \sum_{E_I,\beta} \frac{\langle\alpha;0|V|E_I;\beta\rangle\langle\beta;E_I|V|0;\alpha\rangle}{E_\alpha + i0^+ - (E_I + E_\beta)}. \tag{12.47}$$

Because $V = -(\delta/2)\tau_x\mu$, only terms with $\alpha \neq \beta$ give non-vanishing contributions such that

$$\Sigma_{\alpha\alpha} = \frac{\delta^2}{4} \sum_{E_I} \frac{\langle 0|\mu|E_I\rangle\langle E_I|\mu|0\rangle}{\pm\varepsilon - E_I + i0^+}, \tag{12.48}$$

where $+$ corresponds to $\alpha = \downarrow$, and $-$ to $\alpha = \uparrow$. The diagonal elements of the self-energy in Eq. (12.48) can be cast to the form

$$\Sigma_{\alpha\alpha} = -i\frac{\delta^2}{4}\int_0^\infty dt\, e^{\pm i\varepsilon t} e^{-0^+ t} \langle\mu(t)\mu(0)\rangle. \tag{12.49}$$

To see that (12.49) is equal to (12.48), we first insert a complete set of states of the Ising model, then write the time evolution of μ in the Heisenberg picture, and finally evaluate the integral.

Evaluating Eq. (12.49) with Eq. (12.28) yields

$$\Sigma_{\uparrow\uparrow} = -\frac{\delta^2\Gamma(\frac{3}{4})}{4\varepsilon^{1-2\Delta_\mu}}, \quad \Sigma_{\downarrow\downarrow} = e^{-i\pi/4}\frac{\delta^2\Gamma(\frac{3}{4})}{4\varepsilon^{1-2\Delta_\mu}}, \tag{12.50}$$

where we have used $\varepsilon > 0$. The absence of the imaginary part for $\Sigma_{\uparrow\uparrow}$ indicates that the spin-up state is stable. The self-energy thus gives an energy shift to the spin-up state while it gives an energy shift with a damping to the spin-down state,

$$E_\alpha = \pm\frac{\varepsilon}{2} \mapsto \pm\frac{\varepsilon}{2} + \Sigma_{\alpha\alpha}. \tag{12.51}$$

The energy renormalization and damping (12.51) alter the time evolution of the ground state correlation function

$$\langle\tau^+(t)\tau^-(0)\rangle_0 = e^{-i\varepsilon t} \mapsto e^{-i(\varepsilon+\nu)t-\gamma t/2}, \tag{12.52}$$

where the energy renormalization and damping $\nu - i\gamma/2 \equiv \Sigma_{\downarrow\downarrow} - \Sigma_{\uparrow\uparrow}$ are given by

$$\nu = \frac{\cos^2(\frac{\pi}{8})\Gamma(\frac{3}{4})\delta^2}{2\varepsilon^{1-2\Delta_\mu}}, \qquad \gamma = \frac{\Gamma(\frac{3}{4})\delta^2}{2\sqrt{2}\varepsilon^{1-2\Delta_\mu}}. \tag{12.53}$$

At zero temperature, this correlator is the only non-vanishing qubit correlator that enters in the perturbative calculation. Therefore, the effect of the self energy can be captured by replacing

$$\varepsilon \mapsto \varepsilon + \nu - \tfrac{i}{2}\gamma, \tag{12.54}$$

in the qubit correlation functions computed in the long-time limit excluding the self-energy correction. Using the replacement rule (12.54), one obtains the zero temperature correlator

$$\langle \sigma^x(t)\sigma^x(0)\rangle_c = \frac{e^{-i(\varepsilon+\nu)t-\gamma t/2-i\pi/8}}{t^{2\Delta_\mu}}. \tag{12.55}$$

The energy renormalization and the induced damping (12.51) do not arise explicitly in the lowest-order perturbation and require the resummation of the most divergent contributions to all orders in perturbation theory. In a system where Wick's theorem applies, the resummation for the self-energy can be derived explicitly from a diagrammatic perturbation scheme [267]. Because the correlation functions of multiple μ's do no obey the Wick's theorem (see App. 12.A), the resummation procedure for our system becomes more complicated. In the long time limit, however, the most divergent contributions in all orders can be collected by using the operator product expansion for two μ fields that resembles the structure of the Wick's theorem [241, 248].

12.6.2 Finite temperature

Besides γ, finite temperature is an alternative source of decoherence. The finite temperature correlators of disorder fields are readily obtained from the zero temperature correlators using a conformal transformation [269]:

$$\frac{1}{t^{2\Delta_\mu}} \mapsto \frac{(\pi k_B T)^{2\Delta_\mu}}{[\sinh(\pi k_B T t)]^{2\Delta_\mu}}, \tag{12.56}$$

where T denotes temperature and k_B the Boltzmann constant. The finite temperature correlator $\langle \sigma^x(t)\sigma^x(0)\rangle_c$ in the long-time limit can be obtained by substituting Eq. (12.56) into (12.55) with the proviso $\varepsilon \gg k_B T$ such that the temperature has no direct effect on the qubit dynamics.

12.6.3 Susceptibility

With the correlation functions derived above, we are now in the position to evaluate susceptibilities of the qubit. We should keep in mind that these correlators are valid only in the long-time limit and can only be used to study the behavior of the susceptibilities close to the resonant frequency $\omega \approx \varepsilon$.

Evaluating Eq. (12.32) with Eq. (12.55) yields the susceptibility at zero temperature around the resonance,

$$\chi_{xx}(\omega) = \frac{e^{i3\pi/8}\Gamma(\frac{3}{4})}{[i(\varepsilon+\nu-\omega)+\gamma/2]^{1-2\Delta_\mu}}, \tag{12.57}$$

where ν and γ are given in (12.53). If we neglect ν and γ, which are of higher order in δ/ε, this susceptibility reduces to

$$\chi_{xx}(\omega) = \frac{\Gamma(\frac{3}{4})}{|\omega-\varepsilon|^{1-2\Delta_\mu}} \begin{cases} 1, & \text{for } \omega < \varepsilon, \\ e^{i3\pi/4}, & \text{for } \omega > \varepsilon, \end{cases} \tag{12.58}$$

so it diverges and changes the phase by $3\pi/4$ at the resonant frequency. We can attribute this phase change to the phase shift of the correlator of two disorder fields in Eq. (12.28).

The presence of damping γ in Eq. (12.57) provides a cutoff for the divergence of the response on resonance. The maximal susceptibility is reached at $\omega = \varepsilon + \nu$, and its value is given by

$$|\chi_{xx}(\varepsilon + \nu)| = \frac{2^{1-2\Delta_\mu}\Gamma(\frac{3}{4})}{\gamma^{1-2\Delta_\mu}}. \tag{12.59}$$

Using the proportionality of the correlation functions (12.43) and (12.44), one gets that $\chi_{xz} = \chi_{zx} = -(\delta/\varepsilon)\chi_{xx}$ and $\chi_{zz} = (\delta/\varepsilon)^2\chi_{xx}$. It is interesting to note that when $\delta \to 0$ both χ_{xx} and χ_{xz} are divergent while χ_{zz} vanishes at the resonance.

In Fig. 12.2, the absolute value of the susceptibility $|\chi_{xx}(\omega)|$ close to the resonance is plotted as a function of frequency. The dotted line shows the modulus of Eq. (12.58) for $\nu = \gamma = 0$ while the dashed line shows that of Eq. (12.57). A renormalization of the resonant frequency ν becomes clearly visible when comparing the peak positions of the dashed line to the dotted line.

The conformal dimension of the vortex excitation can be measured in the region with $\varepsilon \gg |\omega - \varepsilon| \gtrsim \gamma$ where

$$|\chi_{xx}(\omega)| = \frac{\Gamma(\frac{3}{4})}{|\omega - \varepsilon|^{1-2\Delta_\mu}}. \tag{12.60}$$

Moreover, both χ_{xz} and χ_{zz} exhibit the same scaling behavior.

The finite temperature susceptibility of $\chi_{xx}(\omega, T)$ can be evaluated from the correlation function (12.55) subjected to the transformation (12.56). The result is plotted as the solid line in Fig. 12.2. An immediate effect of the temperature is that it also introduces a cutoff for the divergence on resonance. For instance, the resonance peak of the susceptibility yields a different scaling behavior with respect to the temperature

$$|\chi_{xx}(\varepsilon + \nu, T)| \propto T^{-(1-2\Delta_\mu)}, \tag{12.61}$$

as long as $\pi k_B T \gg \gamma$. The zero temperature scaling behavior of the resonance peak (12.59) will be masked by a finite temperature with a crossover at $\pi k_B T \approx \gamma$. These scaling and crossover behaviors of the resonance strength are features of the coupling of the Majorana edge states and the flux qubit.

The finite temperature susceptibility shows a resonance at $\varepsilon+\nu$, as shown in Fig. 12.2. Around the resonance, the frequency dependence at finite temperature will be given by the power law (12.60) but with the region constrained by $\pi k_B T$ instead of γ if $\pi k_B T > \gamma$.

12.7 Higher order correlator

So far, we have computed the qubit susceptibilities to their first non-vanishing orders and the lowest order self-energy correction $\varepsilon \mapsto \varepsilon + \nu - i\gamma/2$. As a consequence, we only used the two-point correlation functions $\langle \mu(t)\mu(0)\rangle$ in our evaluations. The next

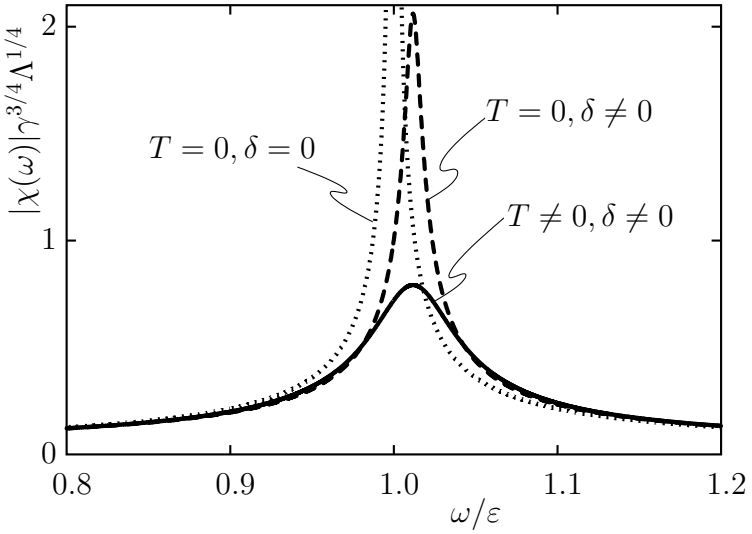

Figure 12.2: Plot of the magnitude of the susceptibility $|\chi_{xx}(\omega)|$ as a function of frequency ω close to resonance ε. The dotted line shows the zero temperature susceptibility in the absence of the damping and energy renormalization while the dashed line shows the result in the presence of the energy shift and the damping in Eq. (12.51). The parameters used for the plot are $\varepsilon = 0.1\Lambda$ and $\delta/\varepsilon = 0.2$. The solid line shows a plot of the finite temperature susceptibility with $k_B T = 0.02\varepsilon$.

nontrivial corrections to the qubit correlators involve the equal position four-point correlator of the disorder fields $\langle\mu(t_1)\mu(t_2)\mu(t_3)\mu(t_4)\rangle$. As discussed in Appendix 12.A, the four-point correlator, in principle, contains information about the non-Abelian statistics of the particles because changing the order of the fields in the correlation function not only alters the phase but can also change the functional form of the correlator [256]. It is thus interesting to go beyond the lowest non-vanishing order. Additionally, doing so allows to check the consistency of the calculation of the self-energy correction done in Sec. 12.6.1.

As an example we focus on the second order correction to the $\langle\sigma^x(t)\sigma^x(0)\rangle_c$ correlator in the long-time limit. The details of the calculation are given in App. 12.B and the result in Eq. (12.108). The dominant correction is a power law divergence

$$\langle\sigma^x(t)\sigma^x(0)\rangle_c^{(2)} \propto e^{-i\pi/8}\frac{e^{-i\varepsilon t}}{t^{2\Delta_\mu}}\left[1-(i\nu+\frac{\gamma}{2})t\right], \tag{12.62}$$

which is just the second order in δ expansion of the modified correlation function

$$\langle\sigma^x(t)\sigma^x(0)\rangle_c \propto \frac{e^{-i(\varepsilon+\nu)t}e^{-\gamma t/2}e^{-i\pi/8}}{t^{2\Delta_\mu}}. \tag{12.63}$$

Hence, we confirm that the second order perturbative correction is consistent with the the self-energy correction calculation.

The leading correction to the susceptibility χ_{xx} in second order is due to the logarithmic term $\propto t^{-1/4}\log t$ in the correlator (12.108) and has the form

$$\chi^{(2)}_{xx}(\omega) = -\frac{\delta^2(2+\sqrt{2})\Gamma(\frac{7}{4})\Gamma(\frac{3}{4})e^{i3\pi/8}}{16\varepsilon^{7/4}[i(\varepsilon+\nu-\omega)+\gamma/2)]^{1-2\Delta_\mu}} \times \ln\left(\frac{(\gamma/2)^2+(\omega-\varepsilon-\nu)^2}{\varepsilon^2}\right) \tag{12.64}$$

where we have included the self-energy correction (12.54), and omitted terms without logarithmic divergence. Unfortunately the effects of nontrivial exchange statistics of disorder fields are not apparent in this correction.

12.8 Conclusion and discussion

We have proposed a novel scheme to probe the edge vortex excitations of chiral Majorana fermion edge states realized in superconducting systems utilizing a flux qubit. To analyze the coupling we mapped the Hamiltonian of the Majorana edge states on the transverse-field Ising model, so that the coupling between the qubit and the Majorana edge modes becomes a local operator. In the weak coupling regime $\delta \ll \varepsilon$ we have found that the ground state expectation values of the qubit spin are given by

$$\langle\sigma^x\rangle = \frac{\Gamma(\frac{3}{4})\delta}{\varepsilon^{1-2\Delta_\mu}\Lambda^{2\Delta_\mu}},\ \langle\sigma^y\rangle = 0,\ \langle\sigma^z\rangle = 1-\frac{3\delta}{8\varepsilon}\langle\sigma^x\rangle. \tag{12.65}$$

Additionally, the susceptibility tensor of the qubit spin in the basis x, y, z is given by

$$\chi(\omega) = \chi_{xx}(\omega)\begin{pmatrix} 1 & 0 & -\delta/\varepsilon \\ 0 & 1 & 0 \\ -\delta/\varepsilon & 0 & (\delta/\varepsilon)^2 \end{pmatrix}, \tag{12.66}$$

$$\chi_{xx}(\omega) = \frac{e^{i3\pi/8}\Gamma(\frac{3}{4})}{[i(\varepsilon+\nu-\omega)+\gamma/2]^{1-2\Delta_\mu}\Lambda^{2\Delta_\mu}}, \tag{12.67}$$

with the real part ν and the imaginary part $\gamma/2$ of the self-energy given by

$$\nu = \frac{\cos^2(\frac{\pi}{8})\Gamma(\frac{3}{4})\delta^2}{2\varepsilon^{1-2\Delta_\mu}\Lambda^{2\Delta_\mu}}, \qquad \gamma/2 = (\sqrt{2}-1)\nu. \tag{12.68}$$

We see that all of these quantities acquire additional anomalous scaling $(\varepsilon/\Lambda)^{2\Delta_\mu}$ due to the fact that each spin flip of the qubit spin couples to a disorder field μ. Similar scaling with temperature appears in interferometric setups [260]. but using a flux qubit allows to attribute its origin to the dynamics of vortices much more easily and also gives additional tunability of the strength of the coupling. Unlike anomalous scaling,

the phase change $\delta\phi = 3\pi/4$ of the susceptibility around the resonance probes the Abelian statistical angle of the disorder field, a feature which cannot easily be measured by electronic means to the best of our knowledge.

The long wavelength theory which we used is only applicable when all of the energy scales are much smaller than the cutoff energy of the Majorana modes. This is an important constraint for the flux qubit coupled to the Majorana edge states. In systems where the time-reversal symmetry is broken in the bulk (unlike for topological insulator-based proposals[2]), the velocity of the Majorana edge states can be estimated to be $v_M \propto v_F \Delta / E_F$ and the dispersion stays approximately linear all the way up to Δ. The cutoff of the Majorana modes is related to the energy scale of the Ising model $\Lambda = \Delta \mapsto J$. Equating $J = \Delta$ and $v_M = 2Ja$, we obtain the lattice constant of the Ising model $a = v_F / E_F \equiv \lambda_F$, with λ_F the Fermi wavelength. The Fermi wavelength is typically smaller than any other length scale, and so the long wavelength approximation we have used is well-justified. For a typical flux qubit the tunneling strength δ is indeed much smaller than the superconducting gap, the level splitting ε may vary from zero to quantities much larger than the superconducting gap.

Our proposal provides a way to measure properties of the non-Abelian edge vortex excitations different from the conventional detection scheme that requires fusing vortices into fermion excitations. However, none of our results for the single flux qubit can be directly connected to the non-Abelian statistics of the quasiparticles, even after including higher-order corrections. Thus, it is of interest for future research to investigate a system where the edge vortex excitations are coupled to two qubits such that braiding of vortex excitations can be probed [8]. Another feature of systems with several qubits worth to investigate is the ability of the Majorana edge modes to mediate entanglement between different flux qubits.

12.A Correlation functions of disorder fields

The one-dimensional critical transverse-field Ising model is a conformal field theory (CFT) with central charge $c = 1/2$. This CFT contains the following primary fields: $\mathbb{I}$, $\epsilon = i\psi\bar{\psi}$, s, and μ. Here $\mathtt{I}$ is the identity operator, ϵ is the energy field (a product of the right and left moving Majorana fermion fields ψ and $\bar{\psi}$), and s is the Ising spin field with its dual field μ [241, 251, 252]. The dual field μ is also called the disorder field and has the same scaling behavior as the Ising spin field s at the critical point. On the lattice, the disorder fields μ are non-linear combinations of Ising spin fields s and reside on the bonds of lattice Ising model. They are hence not independent of the Ising spin field s.

In the continuum and in imaginary time, the two-point correlation function of disor-

[2]For topological insulator-based proposal with time-reversal symmetry in the bulk, cf. Ref. [144], the velocity of Majorana edge modes is further suppressed and is given by $v_M \sim v_F(\Delta/E_F)^2$ when $E_F \gg \Delta$. The cutoff energy for the linear dispersion is constrained to the region $\Lambda \sim \Delta^2/E_F$. In this case, we still get $a = \lambda_F$ the Fermi wavelength.

der fields μ can be obtained from CFT [241]:

$$\langle \mu(z_1, \bar{z}_1)\mu(z_2, \bar{z}_2)\rangle = \frac{1}{[(z_1 - z_2)(\bar{z}_1 - \bar{z}_2)]^{\Delta_\mu}}, \tag{12.69}$$

with $z_i = \tau_i + ix_i$ and $\bar{z}_i = \tau_i - ix_i$.

Following Ref. [256], the real-time correlators can be obtained by analytical continuation $\tau \to \xi + it$. Here $\xi \to 0^+$ is introduced to ensure the correct phase counting and is important for the Abelian part of the statistics. The equal position two-point correlation function is given by

$$\langle \mu(t_1, x_0)\mu(t_2, x_0)\rangle = \frac{1}{(\xi + i(t_1 - t_2))^{2\Delta_\mu}}. \tag{12.70}$$

By using the identity

$$\lim_{\xi \to 0^+} \frac{1}{(\xi + it)^{1/4}} = \frac{e^{-i\,\mathrm{sgn}(t)\pi/8}}{|t|^{1/4}}, \tag{12.71}$$

one obtains the two-point correlation function in the form of Eq. (12.28).

The four-point correlation function of μ's can be obtained in a similar manner. In imaginary time, the correlation function is given by [241]:

$$\langle \mu(z_1, \bar{z}_1)\mu(z_2, \bar{z}_2)\mu(z_3, \bar{z}_3)\mu(z_4, \bar{z}_4)\rangle^2 = \left| \frac{z_{13}z_{24}}{z_{12}z_{34}z_{14}z_{23}} \right|^{1/2} \left(\frac{1 + |\chi| + |1 - \chi|}{2} \right), \tag{12.72}$$

where $\chi = (z_{12}z_{34}/z_{13}z_{24})$ is the conformally invariant cross ratio, and the absolute values should be understood as $|z_{ij}|^\alpha = (z_{ij}\bar{z}_{ij})^{\alpha/2}$. Because we are interested in tunneling at a single point, we can set $x_i = 0$. In this limit the four-point correlation function can be evaluated to be

$$\langle \mu(z_1)\mu(z_2)\mu(z_3)\mu(z_4)\rangle^2 = \begin{cases} \left| \frac{z_{13}z_{24}}{z_{12}z_{34}z_{14}z_{23}} \right|^{1/2} & \text{for} \quad 0 < \chi < 1 \\ \left| \frac{z_{14}z_{23}}{z_{12}z_{34}z_{13}z_{24}} \right|^{1/2} & \text{for} \quad \chi < 0 \\ \left| \frac{z_{12}z_{34}}{z_{14}z_{23}z_{13}z_{24}} \right|^{1/2} & \text{for} \quad \chi > 1 \end{cases} \tag{12.73}$$

The real-time correlation function can be obtained by first taking a square root of

Eq. (12.73) followed by the analytical continuation [256], $\tau_i \to \xi + i t_i$:

$$\begin{aligned}
&\langle \mu(t_1)\mu(t_2)\mu(t_3)\mu(t_4)\rangle \\
&= F_{12}(t_1,t_2,t_3,t_4)\,[\theta(1324)+\theta(1423)+\theta(2413) \\
&\qquad +\theta(2314)+\theta(3241)+\theta(3142)+\theta(4132)+\theta(4231)] \\
&+ F_{13}(t_1,t_2,t_3,t_4)\,[\theta(1234)+\theta(1432)+\theta(2143) \\
&\qquad +\theta(2341)+\theta(3214)+\theta(3412)+\theta(4123)+\theta(4321)] \\
&+ F_{14}(t_1,t_2,t_3,t_4)\,[\theta(1243)+\theta(1342)+\theta(2134) \\
&\qquad +\theta(2431)+\theta(3124)+\theta(3421)+\theta(4213)+\theta(4312)]\,,
\end{aligned} \tag{12.74}$$

where $\theta(abcd) = 1$ for $t_a > t_b > t_c > t_d$ and is otherwise zero. The corresponding functions F_{ij} are given by

$$\begin{aligned}
F_{12}(t_1,t_2,t_3,t_4) &= [\xi + i(t_1-t_2)]^{1/4}[\xi + i(t_3-t_4)]^{1/4}[\xi + i(t_1-t_3)]^{-1/4} \\
&\quad [\xi + i(t_1-t_4)]^{-1/4}[\xi + i(t_2-t_3)]^{-1/4}[\xi + i(t_2-t_4)]^{-1/4},
\end{aligned} \tag{12.75a}$$

$$\begin{aligned}
F_{13}(t_1,t_2,t_3,t_4) &= [\xi + i(t_1-t_3)]^{1/4}[\xi + i(t_2-t_4)]^{1/4}[\xi + i(t_1-t_2)]^{-1/4} \\
&\quad [\xi + i(t_1-t_4)]^{-1/4}[\xi + i(t_2-t_3)]^{-1/4}[\xi + i(t_3-t_4)]^{-1/4},
\end{aligned} \tag{12.75b}$$

$$\begin{aligned}
F_{14}(t_1,t_2,t_3,t_4) &= [\xi + i(t_1-t_4)]^{1/4}[v + i(t_2-t_3)]^{1/4}[\xi + i(t_1-t_2)]^{-1/4} \\
&\quad [\xi + i(t_1-t_3)]^{-1/4}[\xi + i(t_2-t_4)]^{-1/4}[\xi + i(t_3-t_4)]^{-1/4}.
\end{aligned} \tag{12.75c}$$

Here F_{12}, F_{13}, and F_{14} are the three characteristic functions appearing in the fourth-order correlation functions. For an Abelian state, they usually appear in quasi-symmetric combinations and exchanging two of the times alters various phase factors, which is a characteristic of fractional statistics. For the current non-Abelian case, however, exchanging two of the times not only alters phase factors but can also change the form of the correlation function from one of the characteristic functions to another. This is a special feature of non-Abelian statistics [256].

12.B Second order correction to $\langle \sigma^x(t)\sigma^x(0)\rangle_c$

Because our ultimate goal is to compute the qubit susceptibility, we are interested in the correlator with $t > 0$ in the long-time limit $t \to \infty$. Let us first recall the perturbative part of Hamiltonian (12.27) in the interaction picture:

$$V(t,x_0) = -\frac{\delta}{2}\mu(t)[\tau^+(t) + \tau^-(t)]. \tag{12.76}$$

Since the vortex tunneling in or out of the superconducting ring directly couples to the disorder field of the Ising model $\sigma^x(t) = \mu(t)\tau^x(t)$ in the transformed basis, the

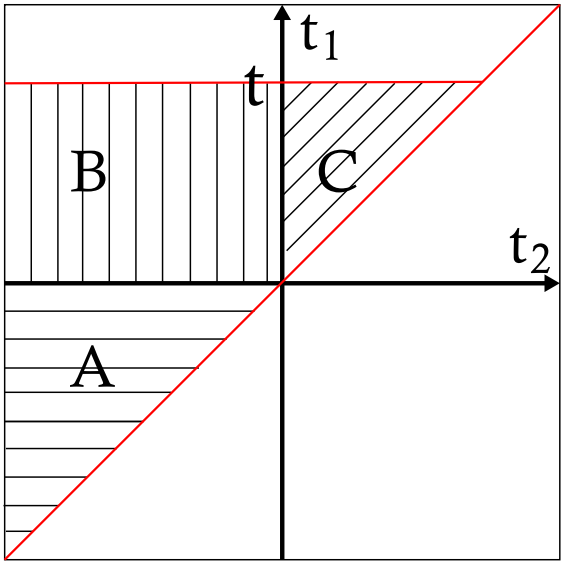

Figure 12.3: The integral domains for regions A, B and C in the t_1 and t_2 coordinates used in Appendix 12.B.

evaluation of the second order correction for the correlator $\langle\sigma^x(t)\sigma^x(0)\rangle$ requires the knowledge of the four-point correlation function derived in Appendix 12.A.

We expand the S and $S^\dagger$-matrices in (12.31) to second order with insertions at times t_1 and t_2. Nonzero contributions to the correlator come from three regions: (A) $t > 0 > t_1 > t_2$, (B) $t > t_1 > 0 > t_2$ and (C) $t > t_1 > t_2 > 0$. These three regions are shown in Fig. 12.3. In what follows, we will evaluate the second order contributions from each region in the long-time limit.

12.B.1 Region A: $t > 0 > t_1 > t_2$

The contribution from region A is given by

$$\langle\sigma^x(t)\sigma^x(0)\rangle_A^{(2)} = (-i)^2 \int_{-\infty}^{0} dt_1 \int_{-\infty}^{t_1} dt_2 I_A, \tag{12.77}$$

with the integrand

$$\begin{aligned} I_A = &+ \langle\sigma^x(t)\sigma^x(0)V_1V_2\rangle_0 + \langle V_2V_1\sigma^x(t)\sigma^x(0)\rangle_0 \\ &- \langle V_2\sigma^x(t)\sigma^x(0)V_1\rangle_0 - \langle V_1\sigma^x(t)\sigma^x(0)V_2\rangle_0, \end{aligned} \tag{12.78}$$

where $V_i \equiv V(t_i)$ is a shorthand notation. The plus and minus signs come from the location of the insertions. The plus sign corresponds to having both insertions located

on the same branch (either forward S or backward $S^\dagger$) while the minus sign corresponds to the situation where the two insertions are located on different branches.

Because only certain orderings of insertions of raising and lowering operators τ^+ or τ^-, coming both from the interaction term (12.76) and the τ^x, give non-vanishing contributions, the integrand is given by

$$\begin{aligned}\left(\frac{2}{\delta}\right)^2 I_A = &+ e^{-i\varepsilon t}e^{i\varepsilon(t_2-t_1)}\langle\mu(t)\mu(0)\mu(t_1)\mu(t_2)\rangle \\ &+ e^{-i\varepsilon t}e^{i\varepsilon(t_1-t_2)}\langle\mu(t_2)\mu(t_1)\mu(t)\mu(0)\rangle \\ &- e^{+i\varepsilon t}e^{i\varepsilon(t_1-t_2)}\langle\mu(t_2)\mu(t)\mu(0)\mu(t_1)\rangle \\ &- e^{+i\varepsilon t}e^{i\varepsilon(t_2-t_1)}\langle\mu(t_1)\mu(t)\mu(0)\mu(t_2)\rangle.\end{aligned} \tag{12.79}$$

Here, the four-point correlation function can be read off from Eq. (12.74) and simplified using the identity (12.71). Remarkably, these correlators have the same time dependence function and differ only by phase factors. This feature is characteristic also to regions B and C. After some algebra, the integrand simplifies to

$$\begin{aligned}I_A = 2\left(\frac{\delta}{2}\right)^2 e^{-i\pi/8}(e^{-i\varepsilon t} - e^{+i\varepsilon t}) \\ \times \mathrm{Re}\left\{e^{i\varepsilon(t_2-t_1)}\frac{(t-t_1)^{1/4}(-t_2)^{1/4}e^{-i\pi/8}}{t^{1/4}(t-t_2)^{1/4}(-t_1)^{1/4}(t_1-t_2)^{1/4}}\right\}.\end{aligned} \tag{12.80}$$

To evaluate the integral (12.77), we first simplify it by introducing new variables such that $t_1 = -tT$ and $t_2 = -t(T+\tau)$ with the new integrating domain $0 < \tau < \infty$ and $0 < T < \infty$. The second order correction from region A becomes

$$\begin{aligned}\langle\sigma^x(t)\sigma^x(0)\rangle_A^{(2)} = it^{3/2}\delta^2 e^{-i\pi/8}\sin(\varepsilon t) \\ \times \mathrm{Re}\left\{e^{-i\pi/8}\int_0^\infty d\tau\frac{e^{-\varepsilon t(\eta+i)\tau}}{\tau^{1/4}}\int_0^\infty dT\frac{e^{-2\eta\varepsilon tT}(1+T)^{1/4}(T+\tau)^{1/4}}{(1+T+\tau)^{1/4}T^{1/4}}\right\},\end{aligned} \tag{12.81}$$

where we have introduced a regularization factor $\exp(\varepsilon\eta t_i)$, with $\eta \to 0^+$.

The integral in Eq. (12.81) will not generate any oscillatory dependence but is divergent when both T and τ are large. It is thus convenient to separate the algebraic part of the integrand into three parts

$$\begin{aligned}I_{A_1} = \frac{(1+T)^{1/4}(T+\tau)^{1/4}}{(1+T+\tau)^{1/4}(T\tau)^{1/4}} - \frac{1}{\tau^{1/4}} - \frac{\tau^{3/4}}{4(T+\tau)(1+T)}, \\ I_{A_2} = \frac{1}{\tau^{1/4}}, \quad I_{A_3} = \frac{\tau^{3/4}}{4(T+\tau)(1+T)}.\end{aligned} \tag{12.82}$$

Combined with the exponential prefactor, the integration of I_{A_1} is regular, the integral of I_{A_2} diverges linearly while that of I_{A_3} diverges logarithmically.

Integrating I_{A_2} with all the exponential prefactors gives

$$\int \frac{e^{-i\pi/8}e^{-\varepsilon t(\eta+i)\tau}e^{-2\eta\varepsilon tT}}{\tau^{1/4}}d\tau dT = \frac{e^{-i\pi/8}\Gamma(\frac{3}{4})}{2\eta(\varepsilon t)^{7/4}(i+\eta)^{3/4}}$$
$$\propto \frac{1}{(\varepsilon t)^{7/4}}[-i\frac{\Gamma(\frac{3}{4})}{2\eta}+\frac{3\Gamma(\frac{3}{4})}{8}+\mathcal{O}(\eta)], \quad \eta\to 0^+ \tag{12.83}$$

Since the the linear long time divergence is purely imaginary, it does not contribute to the correlation function.

In the long-time limit, the integrals of I_{A_1} and I_{A_3} with all the exponential prefactors can be carried out to the lowest order in $1/(\varepsilon t)$ and are given by

$$\int e^{-i\pi/8}e^{-\varepsilon t(\eta+i)\tau}e^{-2\eta\varepsilon tT}I_{A_1}d\tau dT \sim \frac{\Gamma(\frac{7}{4})(\pi-2(1+\log(8)))}{8(\varepsilon t)^{7/4}}, \tag{12.84}$$

$$\int e^{-i\pi/8}e^{-\varepsilon t(\eta+i)\tau}e^{-2\eta\varepsilon tT}I_{A_3}d\tau dT \sim$$
$$-\frac{\Gamma(\frac{7}{4})\left(3\log(8\varepsilon t)-(3\pi/\sqrt{2})e^{-\frac{i\pi}{4}}+3\gamma-4\right)}{12(\varepsilon t)^{7/4}}. \tag{12.85}$$

We now add the real parts of the three integrals (12.83), (12.84), and (12.85) and then multiply them with the prefactors in (12.81). The result is the leading long-time contribution from region A to the qubit spin correlator:

$$\langle\sigma^x(t)\sigma^x(0)\rangle_A^{(2)} \sim$$
$$\frac{\delta^2 e^{-i\pi/8}(e^{i\varepsilon t}-e^{-i\varepsilon t})}{2t^{1/4}\varepsilon^{7/4}}\left\{\frac{\Gamma(\frac{7}{4})(7+3\pi-3\gamma-18\log(2)-3\log(\varepsilon t))}{12}\right\}. \tag{12.86}$$

In the long-time limit, the leading contribution is given by the term $\propto t^{-1/4}\log(\varepsilon t)$.

12.B.2 Region B: $t > t_1 > 0 > t_2$

The contribution from the region B is given by

$$\langle\sigma^x(t)\sigma^x(0)\rangle_B^{(2)} = (-i)^2\int_0^t dt_1\int_{-\infty}^0 dt_2 I_B, \tag{12.87}$$

with the integrand

$$\begin{aligned} I_B = &+\langle\sigma^x(t)V_1\sigma^x(0)V_2\rangle_0+\langle V_2V_1\sigma^x(t)\sigma^x(0)\rangle_0 \\ &-\langle V_2\sigma^x(t)V_1\sigma^x(0)\rangle_0-\langle V_1\sigma^x(t)\sigma^x(0)V_2\rangle_0. \end{aligned} \tag{12.88}$$

After ordering the the raising and lowering operators τ^+ or τ^- and using Eq. (12.74), the integrand reads

$$I_B = e^{-i\pi/4} I_{B_1} + e^{+i\pi/4} I_{B_2} - I_{B_1}^* - I_{B_2}^*, \tag{12.89a}$$

where the two integrand functions are given by

$$I_{B_1} = \frac{\delta^2 e^{-i\varepsilon t} e^{i\varepsilon(t_1+t_2)} t^{1/4}(t_1-t_2)^{1/4}}{4(t-t_1)^{1/4}(t-t_2)^{1/4}(t_1)^{1/4}(-t_2)^{1/4}}, \tag{12.89b}$$

$$I_{B_2} = \frac{\delta^2 e^{-i\varepsilon t} e^{i\varepsilon(t_1-t_2)} t^{1/4}(t_1-t_2)^{1/4}}{4(t-t_1)^{1/4}(t-t_2)^{1/4}(t_1)^{1/4}(-t_2)^{1/4}}, \tag{12.89c}$$

with x^* denoting complex conjugate of x. Again, the four-point correlators of μ's in region B have the same functional form up to phase factors.

To evaluate the integral of I_{B_1}, we introduce new variables x_1 and x_2 with $t_1 = t(1-x_1)$ and $t_2 = -tx_2$ such that

$$B_1 = \int I_{B_1} dt_1 dt_2 = \frac{\delta^2 t^{3/2}}{4} \times \int_0^1 dx_1 \int_0^\infty dx_2 e^{-i\varepsilon t(x_1+x_2)} \frac{(1-x_1+x_2)^{1/4}}{(1-x_1)^{1/4}(1+x_2)^{1/4}(x_1)^{1/4}(x_2)^{1/4}}. \tag{12.90}$$

We can then split the integral B_1 into an oscillatory contribution B_1^O and a non-oscillatory one B_1^{NO}.

Since the non-oscillatory contribution from (12.90) is dominated by $x_1 \sim x_2 \approx 0$, we can expand the integrand around this point to get the leading contribution. Because we are interested in the correlator in the long-time limit, we then deform the integration contour in the complex plane such that both x_1 and x_2 change from 0 to $-i\infty$. The leading non-oscillatory contribution is given by

$$B_1^{NO} \sim \frac{\delta^2 t^{3/2}}{4} \int_0^{-i\infty} dx_1 \int_0^{-i\infty} dx_2 e^{-i\varepsilon t(x_1+x_2)} \left(\frac{1}{(x_1x_2)^{1/4}} + \frac{(x_1x_2)^{3/4}}{4} \right) = \frac{\delta^2 \Gamma(\frac{3}{4})^2 e^{i\pi/4}}{4\varepsilon^{3/2}} \left(-1 + \frac{9}{64\varepsilon^2 t^2} \right). \tag{12.91}$$

The oscillatory contribution B_1^O is dominated by $x_1 \approx 1$ and $x_2 \approx 0$, we can thus expand the integrand around this point to get the leading contribution. Again we are interested in the correlator in the long-time limit and thus deform the integration contour such that x_1 varies from $1 - i\infty$ to 1 and x_2 varies from 0 to $-i\infty$. After these

transformations B_1^O evaluates to

$$B_1^O \sim \frac{\delta^2 t^{3/2} e^{-i\varepsilon t}}{4} \int_{-i\infty}^{0} du_1 \int_0^{-i\infty} dx_2 e^{-i\varepsilon t(u_1+x_2)} \frac{(x_2-u_1)^{1/4}(-u_1)^{1/4}}{u_1 x_2^{1/4}} = \frac{\delta^2 e^{-i\varepsilon t}}{4\varepsilon^{7/4}} \left(\frac{\cos(\frac{\pi}{8})\Gamma(\frac{5}{8})\Gamma(\frac{3}{4})\Gamma(\frac{7}{4})}{\sqrt{2}t^{1/4}\Gamma(\frac{11}{8})} \right), \quad (12.92)$$

where $u_1 = x_1 - 1$.

Summing up, the leading contributions to B_1 are

$$B_1 = \frac{\delta^2}{4\varepsilon^{3/2}} \left\{ \Gamma(\tfrac{3}{4})^2 e^{i\pi/4} \left(\frac{9}{64\varepsilon^2 t^2} - 1 \right) + e^{-i\varepsilon t} \frac{\cos(\frac{\pi}{8})\Gamma(\frac{5}{8})\Gamma(\frac{3}{4})\Gamma(\frac{7}{4})}{\sqrt{2}\Gamma(\frac{11}{8})(\varepsilon t)^{1/4}} \right\}. \quad (12.93)$$

The leading non-oscillatory contribution of B_1 is a constant while the leading oscillatory contribution has a power law decay $\propto t^{-1/4}$.

To integrate I_{B_2}, we again use the variables $t_1 = t(1-x_1)$ and $t_2 = -tx_2$ such that

$$B_2 = \int I_{B_2} dt_1 dt_2 = \frac{\delta^2 t^{3/2}}{4} \times \int_0^1 dx_1 \int_0^\infty dx_2 e^{-i\varepsilon t(x_1-x_2)} \frac{(1-x_1+x_2)^{1/4}}{(x_1)^{1/4}(1+x_2)^{1/4}(1-x_1)^{1/4}(x_2)^{1/4}}. \quad (12.94)$$

Once again, the non-oscillatory contribution is dominated by $x_1 \sim x_2 \approx 0$. We expand the algebraic part of the integrand around $x_1 = x_2 = 0$, deform the integration contour such that x_1 runs from 0 to $-i\infty$ and x_2 from 0 to $i\infty$, and get

$$B_2^{NO} \sim \frac{\delta^2 t^{3/2}}{4} \int_0^{-i\infty} dx_1 \int_0^{i\infty} dx_2 e^{-i\varepsilon t(x_1-x_2)} \left\{ \frac{1}{x_1^{1/4} x_2^{1/4}} + \frac{x_1^{3/4} x_2^{3/4}}{4} \right\} = \frac{\delta^2 \Gamma(\frac{3}{4})^2}{4\varepsilon^{3/2}} \left(1 + \frac{9}{64\varepsilon^2 t^2} \right). \quad (12.95)$$

To evaluate the oscillatory part B_2^O of B_2, we expand the integrand around $x_1 = 1$ and $x_2 = 0$ for the leading contribution. The necessary deformation of the integration contour is now given by x_1 changing from $1 - i\infty$ to 1 and x_2 from 0 to $i\infty$. The leading oscillatory contribution from Eq. (12.94) is now given by

$$B_2^O \sim \frac{\delta^2 t^{3/2}}{4} e^{-i\varepsilon t} \int_{-i\infty}^{0} du_1 \int_0^{i\infty} dx_2 e^{-i\varepsilon t(u_1-x_2)} \left\{ -\frac{(x_2-u_1)^{1/4}(-u_1)^{1/4}}{u_1 x_2^{1/4}} \right\} = \frac{\delta^2 \Gamma(\frac{3}{4})^2}{4\varepsilon^{7/4}} \frac{2\Gamma(\frac{7}{4})}{\sqrt{\pi} t^{1/4}} e^{i\frac{7\pi}{8}} e^{-i\varepsilon t}, \quad (12.96)$$

with $u_1 = x_1 - 1$.

The final expression for B_2 is

$$B_2 = \frac{\delta^2\Gamma(\frac{3}{4})^2}{4\varepsilon^{3/2}}\left(1 + \frac{9}{64\varepsilon^2 t^2} + \frac{2\Gamma(\frac{7}{4})e^{i\frac{7\pi}{8}}}{\sqrt{\pi}(\varepsilon t)^{1/4}}e^{-i\varepsilon t}\right). \tag{12.97}$$

Similarly to B_1, the leading non-oscillatory contribution of B_2 is a constant, while the leading oscillatory contribution has a power law decay $\sim t^{-1/4}$.

From Eq. (12.87) and (12.89), the leading contributions to the qubit spin correlation function from region B is given by

$$\begin{aligned}\langle\sigma^x(t)\sigma^x(0)\rangle_B^{(2)} &= -\left(e^{-i\pi/4}B_1 + e^{i\pi/4}B_2 - B_1^* - B_2^*\right)\\ &= \frac{\delta^2\Gamma(\frac{3}{4})^2}{2\varepsilon^{3/2}}\left(1 - \cos(\pi/4) - \frac{9i\sin(\pi/4)}{64\varepsilon^2 t^2} + \right.\\ &\left.\frac{3\cos(\frac{\pi}{8})\Gamma(\frac{5}{8})}{8\sqrt{2}\Gamma(\frac{11}{8})(\varepsilon t)^{1/4}}(e^{i\varepsilon t} - e^{-i(\varepsilon t+\pi/4)}) + \frac{\Gamma(\frac{7}{4})e^{i\pi/8}}{\sqrt{\pi}(\varepsilon t)^{1/4}}(e^{-i\varepsilon t} - e^{i\varepsilon t})\right).\end{aligned} \tag{12.98}$$

12.B.3 Region C: $t > t_1 > t_2 > 0$

The integral in region C reads

$$\langle\sigma^x(t)\sigma^x(0)\rangle_C^{(2)} = (-i)^2\int_0^t dt_1\int_0^{t_1} dt_2 I_C. \tag{12.99}$$

We calculate the integrand I_C in a similar way to regions A and B. We get

$$I_C = (e^{-i\pi/4} + 1)(I_{C_1} - I_{C_2}), \tag{12.100a}$$

with the two integrand functions being

$$I_{C_1} = \frac{\delta^2 e^{-i\varepsilon t}e^{i\varepsilon(t_1-t_2)}(t-t_2)^{1/4}(t_1)^{1/4}}{4(t-t_1)^{1/4}(t)^{1/4}(t_2)^{1/4}(t_1-t_2)^{1/4}}, \tag{12.100b}$$

$$I_{C_2} = \frac{\delta^2 e^{i\varepsilon t}e^{-i\varepsilon(t_1+t_2)}(t-t_2)^{1/4}(t_1)^{1/4}}{4(t-t_1)^{1/4}(t)^{1/4}(t_2)^{1/4}(t_1-t_2)^{1/4}}. \tag{12.100c}$$

To integrate I_{C_1}, we make the variable transformation: $t_1 = t(T + 1/2 + \tau/2)$ and $t_2 = t(T + 1/2 - \tau/2)$. In terms of the new variables, the integral of I_{C_1} reads

$$\begin{aligned}C_1 = \frac{\delta^2 t^{3/2}e^{-i\varepsilon t}}{4}\int_0^1 d\tau\frac{e^{i\varepsilon t\tau}}{\tau^{1/4}}\int_{-1/2+\tau/2}^{1/2-\tau/2} dT\\ \times\frac{(1/2-T+\tau/2)^{1/4}(1/2+T+\tau/2)^{1/4}}{(1/2-T-\tau/2)^{1/4}(1/2+T-\tau/2)^{1/4}}.\end{aligned} \tag{12.101}$$

The integration over T can be carried out exactly with the result

$$C_1 = \frac{\delta^2 t^{3/2} e^{-i\varepsilon t}}{4} \frac{2\sqrt{\pi}\Gamma(\frac{3}{4})}{\Gamma(\frac{1}{4})} \int_0^1 d\tau \frac{e^{i\varepsilon t\tau}}{\tau^{1/4}} \sqrt{1-\tau^2}\, {}_2F_1\left(-\frac{1}{4}, \frac{1}{2}; \frac{5}{4}; \left(\frac{1-\tau}{1+\tau}\right)^2\right), \quad (12.102)$$

where ${}_2F_1(\alpha, \beta; \gamma; x)$ is the Gaussian hypergeometric function [270].

We deform the integration contour in Eq. (12.102) such that τ goes from 0 to $+i\infty$ and then back from $1 + i\infty$ to 1. The leading contribution in the long-time limit is dominated by the region near the real axis. The expansion around $x = 0$ leads to an oscillatory contribution while the expansion around $x = 1$ leads to a non-oscillatory contribution. To the lowest few orders, the asymptotic behavior in the long-time limit is given by

$$C_1 \sim +\frac{\delta^2 \Gamma(\frac{3}{4})^2 e^{i\pi/4}}{4\varepsilon^{3/2}} \left(-1 + \frac{9}{64\varepsilon^2 t^2}\right) + \frac{\delta^2 e^{-i\varepsilon t}}{4} \left\{ \frac{e^{3i\pi/8}\Gamma(\frac{3}{4}) t^{3/4}}{\varepsilon^{3/4}} + \frac{e^{7i\pi/8}\Gamma(\frac{7}{4})(6\log(\varepsilon t) - (6+3i)\pi + 6\gamma - 14 + 36\log(2))}{12\varepsilon^{7/4} t^{1/4}} \right\}. \quad (12.103)$$

The oscillatory contribution contains a power-law divergent $t^{3/4}$ term. As we discuss later, this term contributes to the shift of the resonant frequency and to the damping for the $\langle \sigma^+(t)\sigma^-(0)\rangle$ correlation function.

To integrate I_{C_2}, we first change the integration variables to τ and T defined by $t_1 = t(T + \tau/2)$ and $t_2 = t(T - \tau/2)$ such that the integral separates into two parts

$$C_2 = \frac{\delta^2 t^{3/2} e^{i\varepsilon t}}{4} \left\{ \int_0^{1/2} dT \int_0^{2T} d\tau + \int_{1/2}^1 dT \int_0^{2-2T} d\tau \right\} \times \left(e^{-i2\varepsilon t T} \frac{(1 - T + \tau/2)^{1/4}(T + \tau/2)^{1/4}}{(1 - T - \tau/2)^{1/4}(T - \tau/2)^{1/4}(\tau)^{1/4}} \right). \quad (12.104)$$

After changing $T \to 1 - T$ in the second integral and then introducing $X = 2T$, this equation simplifies to

$$C_2 = \frac{\delta^2 t^{3/2}}{4} \times \mathrm{Re}\left\{ e^{i\varepsilon t} \int_0^1 dX e^{-i\varepsilon t X} \int_0^X d\tau \frac{(2 - X + \tau)^{1/4}(X + \tau)^{1/4}}{(2 - X - \tau)^{1/4}(X - \tau)^{1/4}(\tau)^{1/4}} \right\}. \quad (12.105)$$

Again, we deform the integration contour in the integral over X with X changing from 0 to $-i\infty$ and then from $1 - i\infty$ to 1. Now the oscillatory contribution comes from

$X \sim 0$ while the non-oscillatory one from $X \sim 1$. By expanding the integrand around these two points, we get the leading contributions:

$$C_2 = \frac{\delta^2\Gamma(\frac{3}{4})^2}{4\varepsilon^{3/2}}\left(1+\frac{9}{64\varepsilon^2 t^2} - \frac{\left(e^{i\varepsilon t}e^{i\pi/8}+e^{-i\varepsilon t}e^{-i\pi/8}\right)}{\varepsilon^{1/4}t^{1/4}}\frac{{}_2F_1\left(-\frac{1}{4},\frac{3}{4};\frac{3}{2};-1\right)\Gamma(\frac{7}{4})}{\sqrt{\pi}}\right). \quad (12.106)$$

The Gaussian hypergeometric function evaluates to ${}_2F_1\left(-\frac{1}{4},\frac{3}{4};\frac{3}{2};-1\right) \approx 1.102$.

From Eqs. (12.99) and (12.100), we obtain contribution to the qubit correlation function from the region C:

$$\begin{aligned}
&\langle\sigma^x(t)\sigma^x(0)\rangle_C^{(2)} = \\
&-(e^{-i\pi/4}+1)(C_1-C_2) \sim \frac{\delta^2\Gamma(\frac{3}{4})^2}{2\varepsilon^{3/2}}\left(1+\cos(\tfrac{\pi}{4})-\frac{9i\sin(\frac{\pi}{4})}{64\varepsilon^2t^2}\right) \\
&+\left(e^{-i\pi/8}\frac{e^{-i\varepsilon t}}{t^{1/4}}\right)\frac{\delta^2\Gamma(\frac{3}{4})}{4\varepsilon^{7/4}}(1+e^{-i\pi/4})(-i\varepsilon t) \\
&+\frac{\delta^2 e^{-i\varepsilon t}e^{-i\pi/8}(e^{-i\pi/4}+1)}{4\varepsilon^{7/4}t^{1/4}}\left\{\frac{\Gamma(\frac{7}{4})(6\log(\varepsilon t)-(6+3i)\pi+6\gamma-14+36\log(2))}{12}\right\} \\
&+\frac{\delta^2\Gamma(\frac{3}{4})^2(e^{-i\pi/4}+1)\left(e^{i\varepsilon t}e^{i\pi/8}+e^{-i\varepsilon t}e^{-i\pi/8}\right)}{4\varepsilon^{7/4}t^{1/4}}\frac{{}_2F_1\left(-\frac{1}{4},\frac{3}{4};\frac{3}{2};-1\right)\Gamma(\frac{7}{4})}{\sqrt{\pi}}.
\end{aligned} \quad (12.107)$$

12.B.4 Final result for $\langle\sigma^x(t)\sigma^x(0)\rangle_c^{(2)}$

The second order correction to the correlation function $\langle\sigma^x(t)\sigma^x(0)\rangle_c^{(2)}$ can be obtained by adding up the contributions from all the three regions, given by Eqs. (12.86), (12.98) and (12.107) and then subtracting $\langle\sigma^x\rangle^2$ as calculated in Eq. (12.40). The full expression

for the correlator in the long-time limit is

$$
\begin{aligned}
&\langle\sigma^x(t)\sigma^x(0)\rangle_c^{(2)} = \\
&-i\frac{9\delta^2\Gamma(\frac{3}{4})^2}{64\varepsilon^{3/2}}\frac{\sin(\frac{\pi}{4})}{\varepsilon^2 t^2}+e^{-i\pi/8}\frac{e^{-i\varepsilon t}}{t^{1/4}}\frac{\delta^2\Gamma(\frac{3}{4})}{4\varepsilon^{7/4}}(1+e^{-i\pi/4})(-i\varepsilon t)\\
&+\frac{\delta^2\Gamma(\frac{7}{4})\log(\varepsilon t)e^{-i\pi/8}}{8\varepsilon^{7/4}t^{1/4}}\left\{(2+e^{-i\pi/4})e^{-i\varepsilon t}-e^{i\varepsilon t}\right\}\\
&-\frac{\delta^2\Gamma(\frac{7}{4})e^{-i\pi/8}e^{-i\varepsilon t}}{4\varepsilon^{7/4}t^{1/4}}\left\{(2+e^{-i\pi/4})\frac{(7+3\pi-3\gamma-18\log(2))}{6}+(e^{i\pi/4}+e^{i\pi/2})\frac{\pi}{4}\right\}\\
&+\frac{\delta^2\Gamma(\frac{3}{4})^2\Gamma(\frac{7}{4})e^{-i\varepsilon t}}{4\varepsilon^{7/4}t^{1/4}}\left(\frac{2e^{i\pi/8}}{\sqrt{\pi}}-\frac{3\cos(\frac{\pi}{8})\Gamma(\frac{5}{8})e^{-i\pi/4}}{4\sqrt{2}\Gamma(\frac{11}{8})\Gamma(\frac{7}{4})}\right.\\
&\qquad\left.+\frac{{}_2F_1\left(-\frac{1}{4},\frac{3}{4};\frac{3}{2};-1\right)(e^{-i3\pi/8}+e^{-i\pi/8})}{\sqrt{\pi}}\right)\\
&+\frac{\delta^2\Gamma(\frac{3}{4})^2e^{i\varepsilon t}}{4\varepsilon^{7/4}t^{1/4}}\left\{\frac{[7+3\pi-3\gamma-18\log(2)]e^{-i\pi/8}}{8\Gamma(\frac{3}{4})}+\frac{3\cos(\frac{\pi}{8})\Gamma(\frac{5}{8})}{4\sqrt{2}\Gamma(\frac{11}{8})}\right.\\
&\qquad\left.-\frac{2\Gamma(\frac{7}{4})e^{i\pi/8}}{\sqrt{\pi}}+\frac{2\cos(\frac{\pi}{8})\,{}_2F_1\left(-\frac{1}{4},\frac{3}{4};\frac{3}{2};-1\right)\Gamma(\frac{7}{4})}{\sqrt{\pi}}\right\}.
\end{aligned}
\tag{12.108}
$$

This result agrees well with numerical evaluation of the integral. A power law divergence $\sim t^{3/4}$ and a logarithmic contribution $\sim \log(\varepsilon t)/t^{1/4}$ dominate the long-time behavior of the correlator. However, this logarithmic contribution will be cut off either by the induced damping or by a finite temperature.

A heuristic way to see that the term diverging as $t^{3/4}$ corresponds to self-energy correction is to add it to the zeroth order correlator of $\langle\sigma^x(t)\sigma^x(0)\rangle$ given by (12.41). The sum of these two terms equals to

$$
\begin{aligned}
&e^{-i\pi/8}\frac{e^{-i\varepsilon t}}{t^{1/4}}\left(1-i\frac{\delta^2\Gamma(\frac{3}{4})}{4\varepsilon^{3/4}}(2\cos^2(\tfrac{\pi}{8})-i\frac{1}{\sqrt{2}})t\right)\\
=&e^{-i\pi/8}\frac{e^{-i\varepsilon t}}{t^{1/4}}\left(1-i(\nu-i\frac{\gamma}{2})t\right),
\end{aligned}
\tag{12.109}
$$

with ν and γ the same as in Eq. (12.51). It then becomes apparent that (12.109) is exactly the expansion of the renormalized correlator (12.55) to the second order in δ

$$
\frac{e^{-i\pi/8}}{t^{1/4}}e^{-i(\varepsilon+\nu)t-\gamma t/2}. \tag{12.110}
$$

We thus conclude that the explicit evaluation of the higher order correction gives a result consistent with the self-energy calculation.

12.B.5 Comments on leading contributions of higher orders

The leading contribution to the second order corrections comes from region C with integration of C_1 when the integration variable τ is around $\tau = 0$, cf. Eq. (12.101). Since $\tau = (t_1 - t_2)/t$, this expansion to the zeroth order is equivalent to making an operator product expansion of $\mu(t_1)\mu(t_2)$ for $t_1 \approx t_2$ in the four-point correlation function of μ operators [241]. In the n^{th} order of perturbation theory with insertion times $t_1, \ldots, t_n$, we expect that the most divergent contribution arises when all the insertion times belong to the interval $[0, t]$. By ordering the times $t_1 > t_2 > \cdots > t_n$ and using the operator product expansion for the pairs $\mu_{t_{2i-1}}\mu_{t_{2i}}$ for $i = 1, \ldots, n/2$, we get a perturbative structure resembling Wick's theorem. The resummation of these terms would give the contributions for the self energy which we calculated in Sec. 12.6.1.